

Increased expression of enolase α in human breast cancer confers tamoxifen resistance in human breast cancer cells

Shih-Hsin Tu · Chih-Chiang Chang · Ching-Shyang Chen · Ka-Wai Tam · Ying-Jan Wang · Chia-Hwa Lee · Hsiao-Wei Lin · Tzu-Chun Cheng · Ching-Shui Huang · Jan-Show Chu · Neng-Yao Shih · Li-Ching Chen · Sy-Jye Leu · Yuan-Soon Ho · Chih-Hsiung Wu

Received: 13 June 2009 / Accepted: 18 July 2009 / Published online: 5 August 2009
© Springer Science+Business Media, LLC. 2009

Abstract Enolase- α (ENO-1) is a key glycolytic enzyme that has been used as a diagnostic marker to identify human lung cancers. To investigate the role of ENO-1 in breast cancer diagnosis and therapy, the mRNA levels of ENO-1 in 244 tumor and normal paired tissue samples and 20 laser capture-microdissected cell clusters were examined by quantitative real-time PCR analysis. Increased *ENO-1* mRNA expression was preferentially detected in estrogen receptor-positive (ER+) tumors (tumor/normal ratio >90-fold) when compared to ER-negative (tumor/normal ratio >20-fold) tumor tissues. The data presented here demonstrate that those patients whose tumors highly expressed *ENO-1* had a poor prognosis with greater tumor size (>2 cm, **P* = .017), poor nodal status (*N* > 3, **P* = .018),

and a shorter disease-free interval (≤ 1 year, **P* < .009). We also found that higher-expressing *ENO-1* tumors confer longer distance relapse (tumor/normal ratio = 82.8–92.4-fold) when compared to locoregional relapse (tumor/normal ratio = 43.4-fold) in postsurgical 4-hydroxy-tamoxifen (4-OHT)-treated ER+ patients (**P* = .014). These data imply that changes in tumor *ENO-1* levels are related to clinical 4-OHT therapeutic outcome. In vitro studies demonstrated that decreasing *ENO-1* expression using small interfering RNA (siRNA) significantly augmented 4-OHT (100 nM)-induced cytotoxicity in tamoxifen-resistant (Tam-R) breast cancer cells. These results suggest that downregulation of *ENO-1* could be utilized as a novel pharmacological approach for overcoming 4-OHT resistance in breast cancer therapy.

Electronic supplementary material The online version of this article (doi:10.1007/s10549-009-0492-0) contains supplementary material, which is available to authorized users.

S.-H. Tu · C.-S. Huang
Department of Surgery, Cathay General Hospital,
Taipei, Taiwan

S.-H. Tu · C.-S. Chen · K.-W. Tam · C.-S. Huang ·
C.-H. Wu (✉)
Department of Surgery, School of Medicine, Taipei Medical
University-Shuang Ho Hospital, No. 252 Wu-Hsing Street,
Taipei 110, Taiwan
e-mail: chwu@tmu.edu.tw

C.-C. Chang · K.-W. Tam · C.-H. Lee · H.-W. Lin ·
T.-C. Cheng · L.-C. Chen · Y.-S. Ho (✉)
Graduate Institute of Medical Sciences, Taipei Medical
University, No. 250 Wu-Hsing Street, Taipei 110, Taiwan
e-mail: hoyuansn@tmu.edu.tw

C.-S. Chen
Center of Quality Management and Breast Health Center, Taipei
Medical University Hospital, Taipei, Taiwan

Y.-J. Wang
Department of Environmental and Occupational Health,
National Cheng Kung University Medical College, Tainan,
Taiwan

J.-S. Chu
Department of Pathology, School of Medicine, Taipei Medical
University, Taipei, Taiwan

N.-Y. Shih
National Institute of Cancer Research, National Health Research
Institutes, Taipei, Taiwan

S.-J. Leu (✉)
Department of Microbiology and Immunology, School
of Medicine, Taipei Medical University, Taipei, Taiwan
e-mail: cmbsycl@tmu.edu.tw

Keywords Tamoxifen · Breast cancer · Enolase-1 · Estrogen receptor alpha · Nuclear factor kappa B

Abbreviations

ChIP	Chromatin immunoprecipitation
DMEM	Dulbecco's modified Eagle's medium
DMSO	Dimethylsulfoxide
E	Estrogens
DOX	Doxorubicin
ENO-1	Enolase α
ENO-2	Enolase β
ENO-3	Enolase γ
ER	Estrogen receptor
FACS	Fluorescence-activated cell sorter
FAS	Fetal calf serum
GAPDH	Glyceraldehyde-3-phosphate dehydrogenase
GF	Griseofulvin
GUS	β -Glucuronidase
IHC	Immunohistochemistry
LCM	Laser capture microdissection
MBP-1	c-Myc promoter-binding protein
MTT	3-(4,5-dimethylthiazol-2-yl)-2,5-diphenyltetrazolium
NF κ B	Nuclear factor kappa B
4-OHT	4-Hydroxytamoxifen
PBS	Phosphate-buffered saline
PDTC	Pyrrolidine dithiocarbamate
PR	Progesterone receptor
PTX	Paclitaxel
RT-PCR	Reverse transcriptase polymerase chain reaction
siRNA	Small interfering RNA
TBP	TATA-box-binding protein

Introduction

Breast cancer is the second leading cause of cancer deaths among women in the United States. In 2005, approximately 215,000 cases of invasive breast cancer (IBC) and 50,000 cases of ductal carcinoma in situ were diagnosed, and 40,000 women died of IBC [1]. The antiestrogen tamoxifen and its active metabolite 4-hydroxytamoxifen (4-OHT) are selective estrogen receptor (ER) modulators that can be used as first-line treatments for ER-positive metastatic breast cancer [2]. However, approximately 40% of patients with ER-positive breast cancer do not respond to tamoxifen treatment [3]. In addition, tamoxifen is usually only effective for a short duration, and most tumors eventually acquire resistance to tamoxifen in 2 to 5 years [4]. Many studies have provided evidence for several different mechanisms that could be involved in the development of

tamoxifen resistance in breast cancer, including *HER2* overexpression [5], altered expression of its co-regulators [5–7], and increased growth factor signaling [6]. However, the precise mechanism of tamoxifen action, especially, in estrogen-dependent cells remains unclear. Therefore, it is important to establish effective techniques for enhancing the efficacy of tamoxifen in the treatment of breast cancer.

Previous studies have demonstrated that human neuroendocrine neuron-specific enolase (ENO) can be used as a marker for in vitro screening of novel anticancer agents [8–11]. ENOs are highly conserved cytoplasmic glycolytic enzymes that catalyze the formation of phosphoenolpyruvate from 2-phosphoglycerate, which generates ATP during glycolysis [8]. Three isoforms of ENO have been identified: ENO- α (ENO-1), ENO- β (ENO-2), and ENO- γ (ENO-3). ENO-1 expression has been detected in nearly all adult human tissues. However, ENO-2 is expressed predominantly in the muscle, and ENO-3 is only expressed in nerve tissues [8]. These three isoforms may exist either as homo- or as heterodimers [12]. ENO-1 is a key glycolytic enzyme that plays a functional role in several physiological processes depending on its cellular localization; it mainly localizes to the cytoplasm, while an alternatively translated form is predominantly localizes to the nuclear region. The nuclear form has been characterized as a c-Myc promoter-binding protein (MBP-1), and it negatively controls transcription [13]. Exogenous expression of MBP-1 inhibits c-Myc transcription [14], while another study demonstrated that both ENO-1 and MBP-1 can bind to the P2 element in the c-Myc promoter and compete with the TATA-box-binding protein (TBP) to suppress transcription of c-Myc [15].

In the present study, *ENO-1* mRNA levels were dramatically increased in surgically dissected (>48-fold, $n = 224$) and laser capture-microdissected (>80-fold, $n = 20$) cell clusters isolated from breast tumor tissues compared to normal cells. In addition, we also demonstrated that nuclear factor kappa B (NF κ B) is involved in the transcriptional activation of ENO-1. Inhibition of *ENO-1* mRNA expression via siRNA knockdown or with the NF κ B pathway inhibitor pyrrolidine dithiocarbamate (PDTC) significantly sensitized tamoxifen-induced cytotoxicity in tamoxifen-resistant (Tam-R) cells. Our results suggest manipulation of ENO-1 as a novel approach for overcoming tamoxifen resistance in breast cancer.

Materials and methods

Cell culture and patient samples

Human breast tumor samples ($n = 244$) were obtained as anonymous specimens from the Taipei Medical University Hospital and from Cathay General Hospital, Taipei,

following a protocol approved by the Institutional Review Board (P950012). ENO-1 immunohistochemical (IHC) analysis was performed using frozen sections from human primary breast tumors. Human mammary gland adenocarcinomas of different ER status (ER+ cells: MCF-7, BT-483; ER– cells: MDA-MB-231, MDA-MB-453, AU-565 cells) and ER– normal human mammary epithelial cell lines (MCF-10A and HBL-100) were purchased from the American Type Culture Collection (Middlesex TW110LY, UK). The cells were grown in the recommended medium (Mediatech, Carlsbad, CA, USA) containing 10% fetal calf serum (FCS; Invitrogen, Carlsbad, CA, USA) and penicillin–streptomycin antibiotics (Mediatech). Tam-R cells derived from MCF-7 cells that were continuously cultured in medium containing 10^{-7} mol/l 4-hydroxytamoxifen (4-OHT, Sigma–Aldrich, Dorset, UK) [16]. The medium for matched control cells contained 0.1% ethanol. Cell proliferation and viability were determined by the 3-(4,5-dimethylthiazol-2-yl)-2,5-diphenyltetrazolium (MTT) assay. An aqueous stock solution of 10 mM doxorubicin (DOX, Chemsyn, Lenexa, KS, USA) and paclitaxel (PTX, Sigma–Aldrich) was prepared in dimethyl sulfoxide (DMSO).

RNA isolation, reverse transcriptase polymerase chain reaction (RT-PCR), and quantitative PCR analysis

Total RNA was isolated from human cell lines and breast tumor tissue samples using TRIzol reagent (Invitrogen). cDNA was amplified from 1 µg of total RNA by SuperScript one-step RT-PCR using the platinum Taq system (Life Technologies, Inc.). The specific primers were synthesized as follows: ENO-1-sense: 5'-CGTACCGCTTCCTTAGA AC-3'; ENO-1-antisense: 5'-GATGACACGAGGCTCAC A-3'; β -glucuronidase (GUS)-sense: 5'-AAACAGCCCG TTTACTTGAG-3'; and GUS-antisense: 5'-AGTGTTCCTGCTAGAATAGATG-3'. A LightCycler thermocycler (Roche Molecular Biochemicals, Mannheim, Germany) was used for real-time PCR. Because real-time RT-PCR is a powerful tool for gene expression analysis, our data were analyzed using GUS that was reported as an ideal control gene with the lowest variability [17] as a control to normalize the expression of the ENO-1 gene. The ENO-1 mRNA fluorescence intensity was measured using built-in Roche LightCycler Software Version 4.

Protein extraction, western blotting, and antibodies

Proteins (50 µg) isolated from breast cancer cells were resolved by 12% SDS–polyacrylamide gel electrophoresis, transferred, and analyzed by western blotting. The following monoclonal antibodies were obtained from various sources as indicated: antiglyceraldehyde-3-phosphate dehydrogenase (GAPDH) and antiENO-1 antibodies (Abcam Inc.,

Cambridge, MA, USA); antiNF κ B (p65), antiER α , and antiER α (p118) antibodies (Santa Cruz Biotechnology, Santa Cruz, CA); and antiMyc antibody (Dako Corporation, Denmark). Alkaline phosphatase-coupled antimouse and antirabbit secondary antibodies were purchased from Santa Cruz Biotechnology.

Preparation of nuclear and cytoplasmic fractions

The NF κ B-specific inhibitor PTDC (Sigma Chemical Co., St. Louis, MO) [17] was added 2 h before 4-OHT treatment. After 24 h of drug treatment, the nuclear and cytoplasmic fractions from control (ethanol-treated) and 4-OHT-treated Tam-R cells were prepared as described previously [18]. The blot was then stripped and reprobed with β -actin or PCNA antibody to ensure equal protein loading and to rule out cross-contamination of cytoplasmic and nuclear fractions (data not shown).

Laser capture microdissection (LCM)

LCM and sample preparation were carried out as described previously [18, 19]. Sections stained using hematoxylin and eosin were subjected to LCM using a PixCell Iie system (Arcturus Engineering, Mountain View, CA). The parameters used for LCM included a laser diameter of 7.5 µm and a laser power of 48–65 mW. For each specimen, 15,000 laser pulse discharges were used to capture 10,000 morphologically normal epithelial cells or malignant cells. The population of cells was visualized under a microscope to ensure that the captured cells were homogeneous. From this group, 20 tumor tissue samples were obtained. In all cases, we were able to obtain individual-matched normal cells. After the cells were captured, total RNA was isolated according to the manufacturer's protocol.

Chromatin immunoprecipitation analysis (ChIP)

ChIP assays from cultured cells were performed as described previously [20]. The NF κ B and ER α antibodies were used for the immunoprecipitation reactions. Primers specific for the detection of transcription factor-binding regions from –694 to –242 of the ENO-1 gene were designed. The sense primer was 5'-AAGAATTATGTC-CAAACCTTCATTCACATA-3', and the antisense primer was 5'-AGTATTCCATTACTGGAACGCT-3'.

ENO-1 gene promoter plasmid construction

The ENO-1 gene promoter region (–1,036 and –1) plasmid was synthesized with PCR primers and linked to a basic luciferase reporter gene in the pGL3 vector (Promega, Madison, WI, USA) with *Kpn I* and *Xho I* restriction

sites. This plasmid was designated as PGL3(*ENO-1*). The pRL-TK vector encodes the *Renilla* luciferase gene, which was used as an internal control to normalize for pGL3 firefly luciferase expression.

Cell culture and dual luciferase reporter assays

MCF-7 (1.5×10^5) cells were washed twice with PBS and mixed with 2 μ g of pGL3(*ENO-1*) and 500 ng of pRL-TK plasmid. Two pulses of 30 ms duration were applied under a fixed voltage of 900 V on a pipette-type microporator, MP-100 (Digital Bio, Seoul, Korea). After 24 h, the cells were transfected in a 6-well plate (5×10^5 /well), and then treated with 4-OHT (10–50 nM). After 24 h of drug treatment, the cells were lysed in passive lysis buffer (Promega). Cell lysates were then added to the luciferase substrate (Dual-Glo luciferase reporter system, Promega), and at the same time, firefly and *Renilla* luciferase activities were measured with a 96-well luminometer (Hidex Chameleon, Finland).

RNA interference

ENO-1 expression was ablated in MCF-7 breast cancer cells using at least two independent small interfering RNAs (siRNAs). siRNAs were chemically synthesized and inserted into a retroviral vector purchased from GenDiscovery Biotechnology, Inc (catalog number: RMM1766-96879192, Taipei, Taiwan). The antisense strand of the siRNA was targeted against *ENO-1* using a 21-nucleotide sequence indicated as Si-1: 5'-GCTGTTGAGCACATCAATAAA-3' and Si-2: 5'-CAGAAACCTTCAAGAGAGGTT-3'. *siENO-1* and scrambled sequence (*scENO-1*) vector constructs were confirmed by DNA sequencing, and BLAST analysis was performed to verify that there was no significant sequence homology with other human genes.

Generation of stable *ENO-1*-knockdown cell lines

The pSUPER-Si-*ENO-1* and the pSUPER-scramble (Sc) vectors were transfected into MCF-7 and Tam-R cells, and stable integrants were selected 72 h later with G418 (4 mg/ml). After 30 days in selective medium, two G418-resistant clones, designated as pSUPER-Si-*ENO-1* (Si-1 and Si-2), were isolated. These clones demonstrated a > 80% reduction in *ENO-1* mRNA and protein levels when compared with the pSUPER-scramble control clones (Sc).

Statistical methods

All data are expressed as means with 95% confidence intervals (CIs) of at least three determinations, unless stated otherwise. A paired *t*-test was used to compare *ENO-1*

mRNA expression in normal vs. tumor paired tissues from breast cancer patients, 4-OHT-induced *ENO-1* promoter activities in MCF-7 cells, and 4-OHT-induced cytotoxic effects in Tam-R cells. The *ENO-1* mRNA expression fold ratios detected in tumor and normal paired samples from surgical or LCM-dissected cells with different clinical staging criteria were compared using the Kruskal–Wallis (nonparametric) test, and each pairwise comparison was made with the Scheffe test. Significant differences in *ENO-1*-knockdown-affected tumor cell proliferation were observed. The expression of *ENO-1* mRNA with clinical factor (ER, PR, HER) parameters was analyzed by the Kruskal–Wallis (nonparametric) test, and each pairwise comparison was made with the Mann–Whitney test. All statistical comparisons were performed using SigmaPlot graphing software (San Jose, CA), and the Statistical Package for the Social Sciences v.11.0.0 (SPSS, Chicago, IL). A *P*-value of < 0.05 was considered to be statistically significant, and all statistical tests were two-sided.

Results

Increased mRNA expression of *ENO-1* in human breast tumor tissues

ENO-1 is a key glycolytic enzyme and has been used as a diagnostic marker to identify human lung cancers [21–23]. To investigate the role of *ENO-1* in breast cancer carcinogenesis, the mRNA levels of *ENO-1* in 244 breast tumor and normal paired tissue samples were examined by quantitative PCR (Fig. 1a–d) and RT-PCR (Supplementary Fig. S1) analyses. The *ENO-1* PCR amplification curves in tumor tissues (Fig. 1a, red lines) were significantly “left-shifted” compared to the profiles of normal tissues (Fig. 1a, green lines). Real-time PCR results were calculated, and tissues were divided into two groups according to their level of *ENO-1* mRNA expression. More than two-thirds ($n = 165$) of the tissues fell into group 1 (tumor > normal), for which the average *ENO-1* expression level in tumor cells was >48-fold higher than that of normal cells (Fig. 1b, $*P < 0.001$). In contrast, the expression level of *ENO-1* in most normal tissues (55/79) in group 2 (normal > tumor) was less profound than in tumor tissues (Fig. 1b, bars 3 vs. 4, $\#P = < 0.05$; Fig. 1c, bars 5–7). *ENO-1* expression in human breast tumors was not correlated with their diagnostic stage (Fig. 1d). A significant increase in *ENO-1* protein expression was detected by IHC staining of tumor tissues that were diagnosed as invasive ductal and lobular carcinomas (IDC) (Fig. 1e, upper panel, red square frame, indicated by yellow arrows). In contrast, normal tissues did not express significant levels of *ENO-1* (Fig. 1e, upper panel, green square frame, indicated by the green arrows).

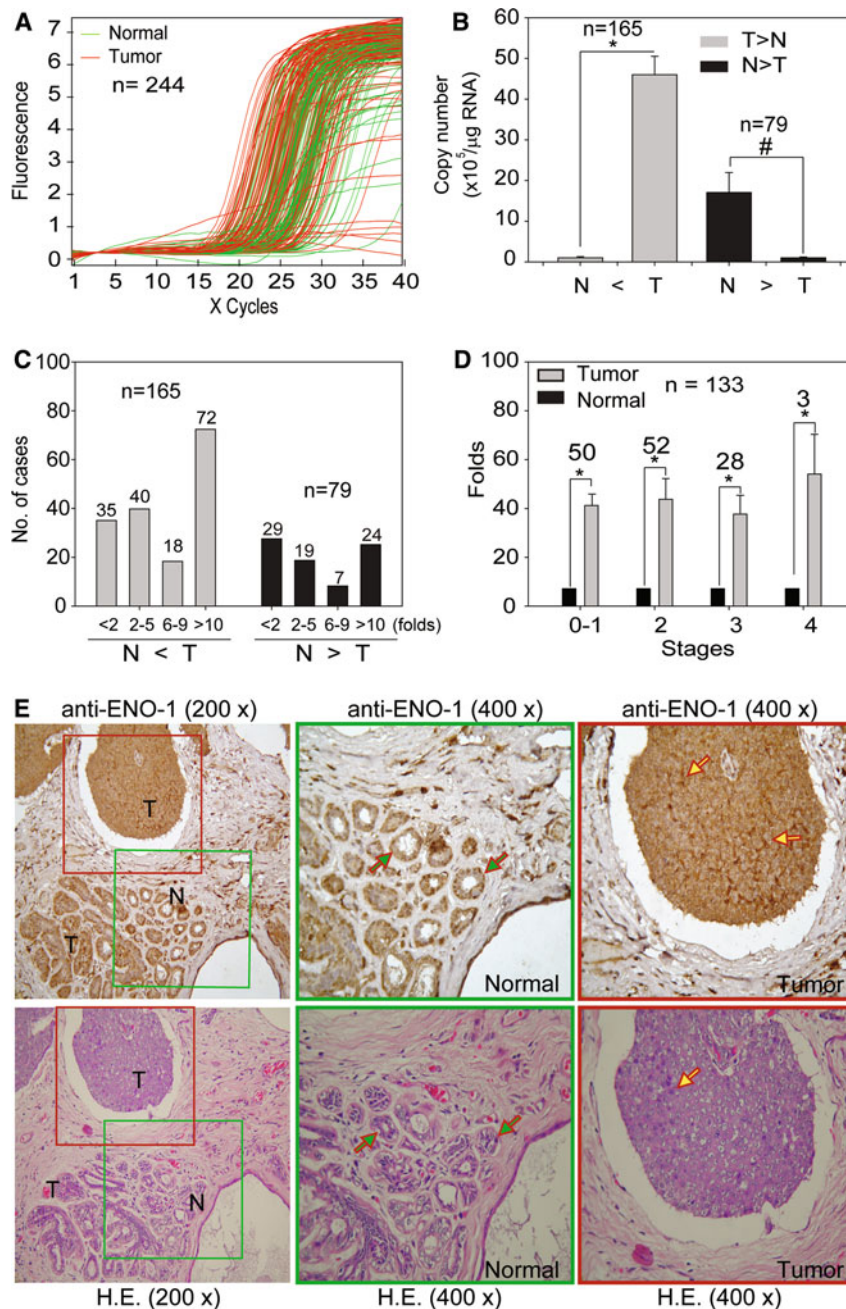


Fig. 1 ENO-1 overexpression in human breast tumor tissues. **a** Real-time PCR amplification curves showing ENO-1 mRNA expression profiles in human breast tumor (red lines) and normal (green lines) tissues ($n = 244$). **b** The average ENO-1 mRNA expression level in paired human breast tissues was calculated by real-time PCR. T, tumor; N, normal. Data are presented as the mean of the ENO-1 mRNA expression level, which is presented as copy number ($\times 10^5$ per μg RNA); error bars are 95% confidence intervals. * represents normal vs. tumor tissue in group 1, $P < 0.001$; # represents normal vs. tumor tissue in group 2, $P < 0.05$. Data were analyzed using paired t -tests, and all P -values are two-sided. **c** The ENO-1 mRNA levels calculated in Fig. 1b were subdivided into four groups (< 2, 2–5, 6–9, and >10-fold). The case numbers are presented. **d** ENO-1 mRNA

levels in breast tumor and normal tissues were divided into four subgroups according to their clinical staging criteria as suggested by the American Journal of Critical Care (AJCC). Data were analyzed using paired t -tests, and all P -values are two-sided. * represents normal vs. tumor tissue in group 1, $P < 0.001$; data are presented as the mean fold ratio for the comparison of paired tumor and normal tissues; error bars are 95% confidence intervals. The comparisons were carried out as follows: stage 0–1 vs. stage 2, $P = 0.76$; stage 0–1 vs. stage 3, $P = 0.47$; stage 0–1 vs. stage 4, $P = 0.76$. Data were analyzed by an overall nonparametric test (Kruskal–Wallis test), and multiple comparisons were assessed by the Scheffe test; all P -values are two-sided. **e** Immunolocalization of ENO-1 protein expression in human IDC breast tumor tissues

The morphology of the tumor cells was confirmed by hematoxylin and eosin staining and defined according to clinical criteria (Fig. 1e, lower panels).

Increased mRNA expression of ENO-1 in ER+ tumor tissues

To ascertain ENO-1 expression levels in human breast tumor tissues and their implications for clinical diagnostic purposes, patients were categorized according to their ER, progesterone receptor (PR), and HER-specific staining results. In groups 1 and 2, ENO-1 expression was preferentially detected in ER+ patients compared to ER- patients (Fig. 2a, $**P < 0.01$). In contrast, ENO-1 expression in PR+ vs. PR- tumor tissues was less profound (Fig. 2a, $*P < 0.05$). We further determined whether higher ENO-1 mRNA expression levels were correlated with ER+ tumor tissues. Increased ENO-1 mRNA expression was detected in ER+ (>90-fold) tumors when compared to ER- (>20-fold) tumors (Fig. 2b, bars 1 vs. 2, $**P < 0.01$). Thus, higher ENO-1 expression was closely related to ER+ human breast tumor tissues. To confirm these observations, LCM was performed, and tumor and normal cell clusters were harvested separately from 20 different tumor samples (Fig. 2c). Increased expression of ENO-1 was detected in LCM-dissected ER+ tumor cells (Fig. 2d, bar 2 vs. 4, $*P < 0.01$ and $\#P = 0.001$).

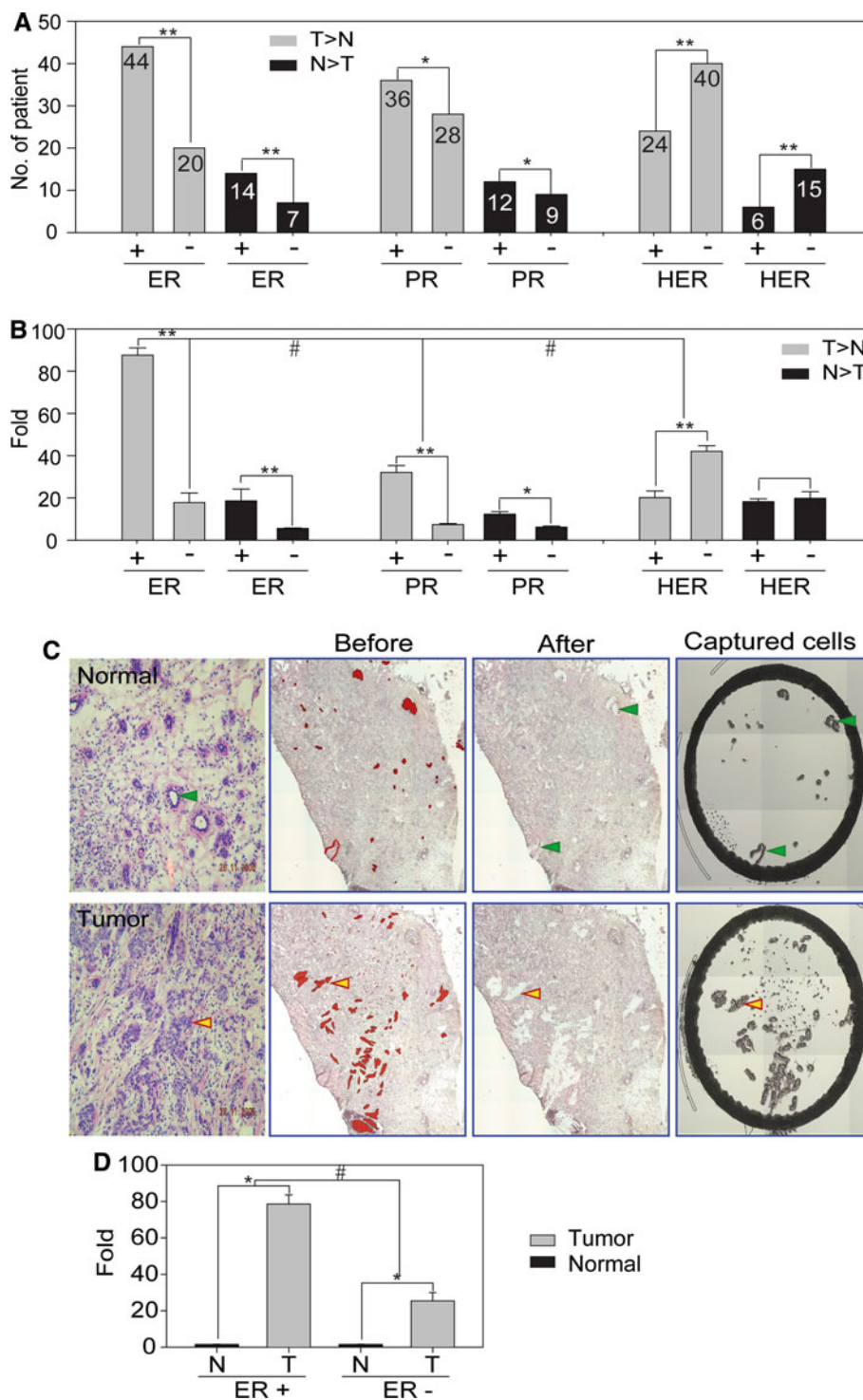
To further evaluate whether the higher expression levels of ENO-1 detected in ER+ tumors were related to clinical therapeutic outcome, 51 cases of ER+ patients treated with postsurgical 4-OHT chemotherapy were selected, and the clinical status of each was determined. The data presented here demonstrate that those patients whose tumors highly expressed ENO-1 had a poor prognosis with greater tumor size (>2 cm, $*P = 0.017$), poor nodal status ($N > 3$, $*P = 0.018$), and a shorter disease-free interval (≤ 1 year, $*P < 0.009$) (Table 1). We also found that a higher expression level of ENO-1 (T/N ratio = 82.8–92.4 fold) conferred longer distance relapse when compared to locoregional relapse (T/N ratio = 43.4-fold) in 4-OHT-treated ER-positive patients ($*P = 0.014$) (Table 1). Such results imply that higher expression levels of ENO-1 in breast tumor tissues are related to the clinical outcome of 4-OHT therapeutic resistance.

ENO-1 expression was inducible in the 4-OHT-treated MCF-7 (ER ±) cells

To further investigate the carcinogenic role of ENO-1 expression involved in the proliferation of human breast cancer cells, the ENO-1 protein expression profile was evaluated in human breast cancer (BT-483, MDA-MB-453, MDA-MB-231, AU-565, and MCF-7) and normal mammary

Fig. 2 ENO-1 gene expression is associated with ER-positivity in breast tumor tissues. **a** The case numbers for ENO-1 mRNA expression detected in human breast tumor tissues were correlated with staining for ER, PR, and HER. Data were analyzed using paired *t*-tests; all *P*-values are two-sided. ****** represents ER+ vs. ER- and HER+ vs. HER-, $P < 0.01$; ***** represents PR+ vs. PR-, $P < 0.05$. **b** ENO-1 mRNA expression levels detected by real-time PCR were correlated with clinical diagnostic markers in these tumor tissues. Data were analyzed using paired *t*-tests; all *P*-values are two-sided. The data are presented as the mean fold ratios for the comparisons of ER ± vs. ER-, PR ± vs. PR-, and HER ± vs. HER- tissues; *error bars* are 95% confidence intervals ($*P < 0.05$, $**P < 0.01$). Comparisons were further performed in ER +/ER- vs. PR +/PR-, $\#P = 0.01$; and ER +/ER- vs. HER +/HER-, $\#P = 0.02$. Data were analyzed using a nonparametric test (Kruskal–Wallis and Mann–Whitney test); all *P*-values are two-sided. **c** Hematoxylin and eosin-stained tumor tissue sections from representative cases with normal (*upper*) and tumor (*lower*) cells prior to microdissection (*left panels*). The cells shown here were selectively captured and transferred to the film on the LCM cap (*right panels*). *Green arrowheads*: laser imprint showing captured normal cells; *yellow arrowheads*: tumor cells. Magnification, 20×. **d** The ENO-1 mRNA expression level in the LCM-captured cells was detected by real-time PCR analysis. The ER+ group was significantly different from the ER- group. Data were analyzed using paired *t*-tests; all *P*-values are two-sided. ($*P < 0.01$). Data are presented as the mean fold ratios for the comparison of paired normal vs. tumor tissues; *error bars* are 95% confidence intervals. The comparison was carried out as follows: ER+ group vs. ER- group, $\#P = 0.001$. Data were analyzed by an overall nonparametric test (Kruskal–Wallis test); all *P*-values are two-sided

(MCF-10A and HBL-100) cells with varying ER status (Fig. 3a). Surprisingly, the ENO-1 protein expression was less profound in ER ± (MCF-7 and BT-483) cells when compared to ER- (MDA-MB-231) cells. These results were inverse to the results obtained from tumor tissues as described earlier (Fig. 2a and b). Therefore, we wondered whether ENO-1 expression in the ER ± cells could be induced in response to chemotherapeutic agents. To test this hypothesis, MCF-7 (ER ±) cells were treated with various concentrations of anticancer agents (4-OHT, PTX and DOX). The doses for 4-OHT, DOX, and PTX ($IC_{50} = 10, 0.42, \text{ and } 0.83 \mu\text{M}$, respectively) used in MCF-7 cells were selected according to previous studies [24–26]. In the present study, we reduced the concentrations of these agents proportionally by 1,000-fold, which caused noncytotoxic effects on MCF-7 cells. We also treated the MCF-7 cells with griseofulvin (GF), an antifungal agent that acts on microtubules in a similar mechanism to PTX [27]. The results demonstrate that only 4-OHT-induced ENO-1 protein expression was detected in MCF-7 cells (Fig. 3b). To further investigate whether ENO-1 induction by 4-OHT treatment was cell type-specific, the MCF-7 (ER ±) and MDA-MB-231 (ER-) cells were treated with 4-OHT at varying doses. We found that ENO-1 protein expression was easily induced by 4-OHT ($\geq 50 \text{ nM}$) treatment in MCF-7 cells but not in MDA-MB-231 cells (Fig. 3c).



ENO-1 upregulation confers 4-OHT resistance to human breast cancer cells

We next tested whether ENO-1 induction in MCF-7 cells treated with lower concentrations (< 100 nM) of 4-OHT conferred drug-induced resistance. In support of this

hypothesis, long-term (> 12 month) treatment with 4-OHT (100 nM) resulted in the selection of proliferating resistant colonies, and a tamoxifen-resistant MCF-7 (designed as Tam-R) cell line was generated [16]. The ENO-1 protein level in MCF-7 and Tam-R cells exposed to 4-OHT was determined by immunoblotting assays. The ENO-1

Table 1 ENO-1 levels and correlation of clinical outcomes after first-line 4-OHT treatment of patients with estrogen receptor-positive primary breast tumors

Characteristics	(n)	Tumor > normal			Normal > tumor		
		(n)	Fold	Tumor vs. normal (P)	(n)	Fold	Normal vs. tumor (P)
Patients (total number)	244	165	44.4 ± 3.5	<i>P</i> < 0.001 ^a	79	16.8 ± 2.7	<i>P</i> < 0.01 ^a
4-OHT therapy	51 ¹	45	80.4 ± 1.5	<i>P</i> < 0.001 ^a	6	19.3 ± 3.8	<i>P</i> < 0.01 ^a
Age at start of therapy		<i>n</i> (%)			<i>n</i> (%)		
≤40		5 (11.1)	51.8 ± 4.5	<i>P</i> < 0.001 ^a	2 (33.3)	19.2	ND
41–55		14 (31.1)	71.4 ± 6.1	<i>P</i> < 0.001 ^a	3 (50)	18.2	ND
56–70 ²		24 (53.3)	93.4 ± 9.2	<i>P</i> < 0.001 ^a	1(16.6)	22.3	ND
>70		2 (4.4)	63.4 ± 4.8	ND	0	0	ND
Disease-free interval (years)		<i>n</i> (%)			<i>n</i> (%)		
≤1 ³		9 (20)	119.4 ± 6.8	<i>P</i> < 0.0015 ^a	1 (7.6)	18.5 ± 2.1	ND
1–3		28 (62.2)	80.1 ± 2.2	<i>P</i> < 0.001 ^a	2 (33.3)	22.5 ± 1.8	ND
>3		8 (17.7)	37.7 ± 3.5	<i>P</i> < 0.018 ^a	3 (50)	17.2 ± 1.7	ND
Dominant site of relapse 17		<i>n</i> (%)					
Locoregional ⁴		3 (17.6)	43.4 ± 5.6	<i>P</i> < 0.013 ^a	ND		
Bone		8 (47)	82.8 ± 2.8	<i>P</i> < 0.001 ^a	ND		
Viscera		6 (35)	92.4 ± 5.1	<i>P</i> < 0.001 ^a	ND		
Nodal status		<i>n</i> (%)			<i>n</i> (%)		
<i>N</i> 0		22 (48.8)	60.9 ± 2.1	<i>P</i> < 0.001 ^a	5 (83.3)	21.1 ± 7.1	<i>P</i> < 0.001 ^a
<i>N</i> 1–3		11 (24.4)	91.8 ± 3.8	<i>P</i> < 0.001 ^a	1 (16.6)	10.1	ND
<i>N</i> > 3 ⁵		11 (24.4)	98.4 ± 5.1	<i>P</i> < 0.001 ^a	ND	ND	
Unknown		1 (2.2)	188		ND	ND	
Tumor size		<i>n</i> (%)			<i>n</i> (%)		
≤2 cm ⁶		25 (55.5)	69.8 ± 5.3	<i>P</i> < 0.001 ^a	5 (83.3)	18.9 ± 4.1	ND
>2 cm		20 (44.4)	93.65 ± 3.7	<i>P</i> < 0.001 ^a	1 (16.6)	21.3 ± 1.3	ND
Tumor grade		<i>n</i> (%)			<i>n</i> (%)		
Poor		14 (31.1)	78.9 ± 7.2	<i>P</i> < 0.001 ^a	2 (33.3)	17.2 ± 3.3	ND
Unknown		18 (40)	88.2 ± 3.1	<i>P</i> < 0.001 ^a	4 (66.6)	20.35 ± 3.3	ND
Good/moderate		13 (28.8)	71.2 ± 5.8	<i>P</i> < 0.001 ^a	ND		

ND not determined

¹ Tumor > Normal vs. Normal > Tumor, *P* = 0.013^b

² 56–70 vs. ≤40, *P* = 0.019^b

³ ≤1 year vs. > 3 year, *P* < 0.009^b

⁴ Locoregional vs. bone, *P* = 0.014^b

⁵ *N* > 3 vs. *N* 0, *P* = 0.018^b

⁶ ≤2 cm vs. >2 cm, *P* = 0.017^b

^a Paired *t*-test

^b Mann–Whitney test

expression level was higher in Tam-R cells when compared to MCF-7 cells in the presence of 4-OHT treatment (Fig. 4a, lane 2). These results imply that ENO-1 induction is closely

related to 4-OHT resistance in Tam-R cells. Although the cellular proto-oncogene *c-Myc* was originally reported to be involved in cellular transformation, it has also been

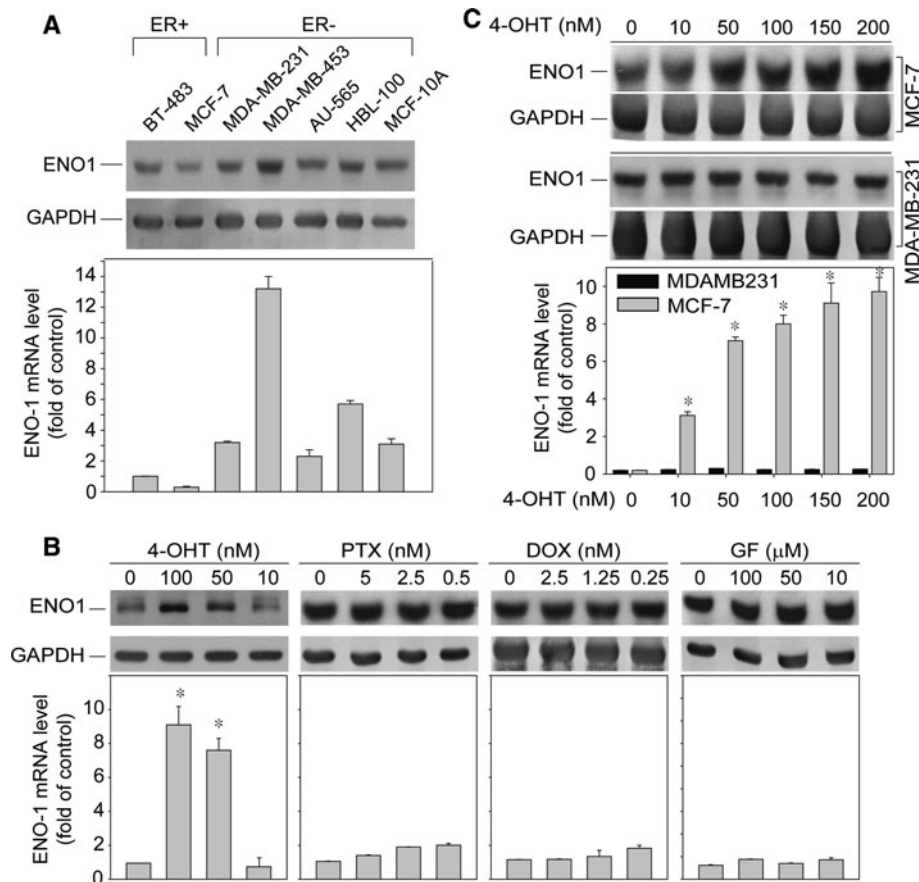


Fig. 3 Protein and mRNA expression of ENO-1 is induced in 4-OHT-treated MCF-7 cells. **a** The basic ENO-1 protein and mRNA expression profiles of normal and malignant mammary cell lines were detected by immunoblot (*upper panel*) and real-time PCR (*lower panel*) assays. The ENO-1 mRNA level in BT-483 cells (*bar 1*) is shown as the baseline level. Data shown here are indicated as fold of control by comparison between BT-483 and all other cell lines. **b** MCF-7 cells were treated with different anticancer agents in a concentration-dependent manner. After 24 h of drug treatment, ENO-1 protein and mRNA expression levels were assessed by immunoblot and real-time PCR analysis. The ENO-1 mRNA level in cells treated with vehicle alone (*bar 1*, in each group) is shown as the baseline

level. Data shown here are shown as fold of control by comparison between drug- vs. vehicle-treated groups. Data were analyzed using paired *t*-tests; all *P*-values are two-sided. ($*P \leq 0.01$). **c** MCF-7 (ER+) and MDA-MB-231 (ER-) cells were treated with 4-OHT at varying concentrations. Protein and mRNA expression levels were detected by immunoblot (*upper panel*) and real-time PCR (*lower panel*) assays. The ENO-1 mRNA level in cells treated with vehicle alone (*bars 1 and 2*) is shown as the baseline level. Data shown here are shown as fold of control by comparison between 4-OHT- vs. vehicle-treated groups. Data were analyzed using paired *t*-tests; all *P*-values are two-sided. ($*P \leq 0.01$). PTX: paclitaxel, DOX: doxorubicin, GF: griseofulvin

implicated in antitumor drug-induced apoptosis [28]. Therefore, we hypothesized that ENO-1 (or MBP-1)-mediated c-Myc downregulation [15, 29, 30] may be a mechanism by which breast cancer cells acquire resistance to 4-OHT-induced apoptosis. To test this hypothesis, c-Myc protein levels were measured and found to be downregulated in Tam-R and MCF-7 cells upon treatment with a lower dose of 4-OHT (100 nM) (Fig. 4a, lanes 2 and 4).

To further explore whether c-Myc expression correlated with ENO-1 protein changes that confer 4-OHT resistance to breast cancer cells, we generated a stable Tam-R cell line in which ENO-1 was knocked down using RNA interference (siRNA, designated as Tam-R-Si cells). In the present study, the data shown in Fig. 4b, lanes 3–4, were selected from two different ENO-1 siRNA clones (designed as Si-1, and Si-2)

targeted to independent parts of the enolase mRNA. Reduced levels of ENO-1 protein and mRNA were detected in the stable cell lines (Fig. 4b, lanes 3 and 4). The Tam-R-Si and Tam-R-Sc cells were treated with or without 4-OHT (100 nM) for 24 h. (Fig. 4c). In the 4-OHT-treated Tam-R-Si cells, c-Myc expression was significantly induced compared to the Tam-R-Sc control cells (Fig. 4c, lanes 1 vs. 2). In contrast, c-Myc protein induction in the vehicle control cells was less profound (Fig. 4c, lanes 3 and 4). Such results indicate that c-Myc expression is inversely related to ENO-1 expression in Tam-R cells in response to 4-OHT treatment. The c-Myc signaling proteins have been demonstrated to be involved in 4-OHT-induced apoptosis in human breast cancer cells [30–32]. Accordingly, to test whether the upregulation of c-Myc protein sensitized Tam-R-Si cells to

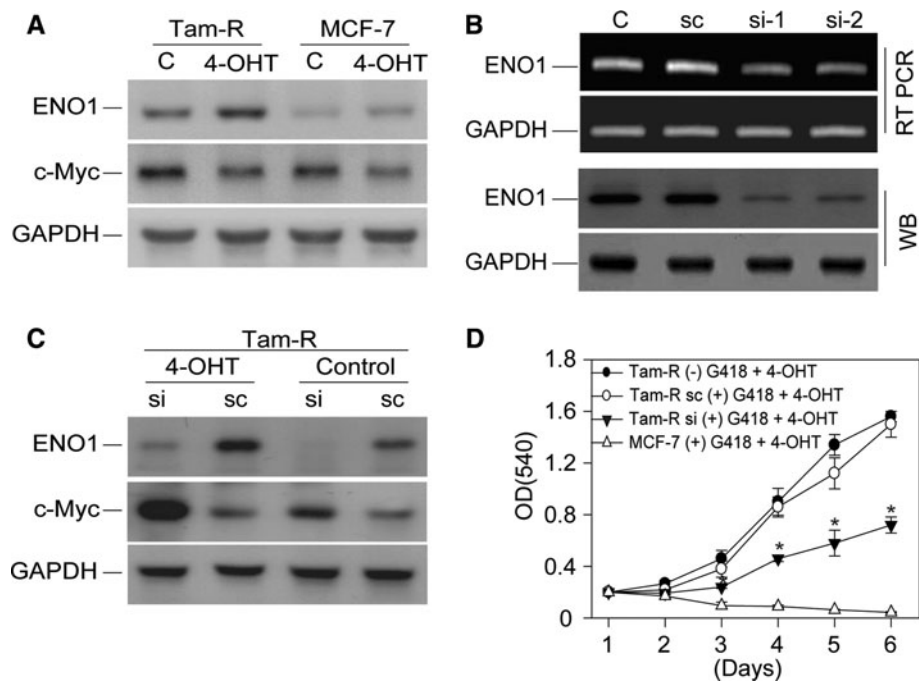


Fig. 4 ENO-1 protein is upregulated for 4-OHT-resistance in human breast cancer cells. **a** Human MCF-7 and Tam-R cells were treated with 4-OHT (100 nM) for 24 h to determine the changes in ENO-1 and c-Myc protein expression. Cells treated with vehicle alone were used as a control (indicated as *c*). **b** Stable ENO-1-knockdown (Tam-R-Si) and scramble sequence control (Tam-R-Sc) cell lines were generated by G418 (4 mg/ml) medium selection. Protein and mRNA expression levels were detected by immunoblot and RT-PCR analysis. **c** Tam-R cells with stable ENO-1 knockdown (Tam-R-Si) were treated in the presence or absence of 4-OHT (100 nM) for 24 h. Cells transfected with the scramble (Tam-R-Sc) sequence plasmid were used as a control. Protein expression levels of ENO-1 and c-Myc were detected

by immunoblot analysis. **d** Established Tam-R cell lines with stable ENO-1-knockdown (Tam-R-Si) and scramble control (Tam-R-Sc) were cultured in G418 medium (4 mg/ml) with 4-OHT (100 nM) for 1–6 days. The Tam-R cells treated with 4-OHT alone and MCF-7 cells treated with G418 plus 4-OHT were used as controls. Cell growth in each group was measured using an MTT assay. Data are presented as means; error bars are 95% confidence intervals. For statistical analysis, Tam-R-Si cells with G418 selection (▼) were compared to either Tam-R-Sc cells with G418 selection (○), Tam-R cells without G418 selection (●), or wild type MCF-7 cells with G418 selection (△), * $P = 0.009$. The data were analyzed by nonparametric tests (Kruskal–Wallis and Mann–Whitney tests); all P -values are two-sided

4-OHT treatment, a cell growth proliferation assay was performed. Surprisingly, the antiproliferative effect of 4-OHT was significantly augmented in Tam-R-Si (presented as a “▼” symbol) cells when compared to Tam-R-Sc (presented as a “○” symbol) cells (Fig. 4d, * $P = 0.009$).

4-OHT-induced ENO-1 transcriptional upregulation through activation of ER α or NF κ B in MCF-7 cells

There are many putative transcription factor-responsive elements located in the promoter of ENO-1 (Fig. 5a). To evaluate ENO-1 promoter activity, which is regulated by 4-OHT-induced transcription factors, the ENO-1 gene promoter was cloned into the luciferase reporter plasmid pGL3(ENO-1). Experiments utilizing this construct demonstrated that ENO-1 promoter activity was significantly induced by 4-OHT (10–50 nM, for 6 h.) in MCF-7 cells (Fig. 5b, * $P < .05$). We first determined the changes in ER α , which is activated by specific phosphorylation of a serine residue (Ser-118) in Tam-R cells [33–35]. Our

results demonstrated that ENO-1, ER α , and P-Ser(118)-ER α were consistently induced in MCF-7 cells following 4-OHT treatment (Fig. 5c). We also demonstrated that NF- κ B was responsible for ENO-1 induction based on examination of nuclear and cytosolic extracts prepared from 4-OHT-treated MCF-7 cells. Increased nuclear translocation of NF- κ B from the cytosol was detected by immunoblotting (Fig. 5c, lanes 3–4), and direct evidence of increased DNA binding either by ER α or by NF κ B to the ENO-1 promoter was demonstrated by ChIP analysis in 4-OHT-treated MCF-7 cells (Fig. 5d, lane 2). These results imply that either P-Ser(118)-ER α or NF κ B was activated to act as a transcriptional factor in 4-OHT-induced ENO-1 upregulation.

Inhibition of ENO-1 expression sensitizes Tam-R cells to 4-OHT treatment

In the present study, inhibition of ENO-1 protein expression by siRNA knockdown in Tam-R cells significantly

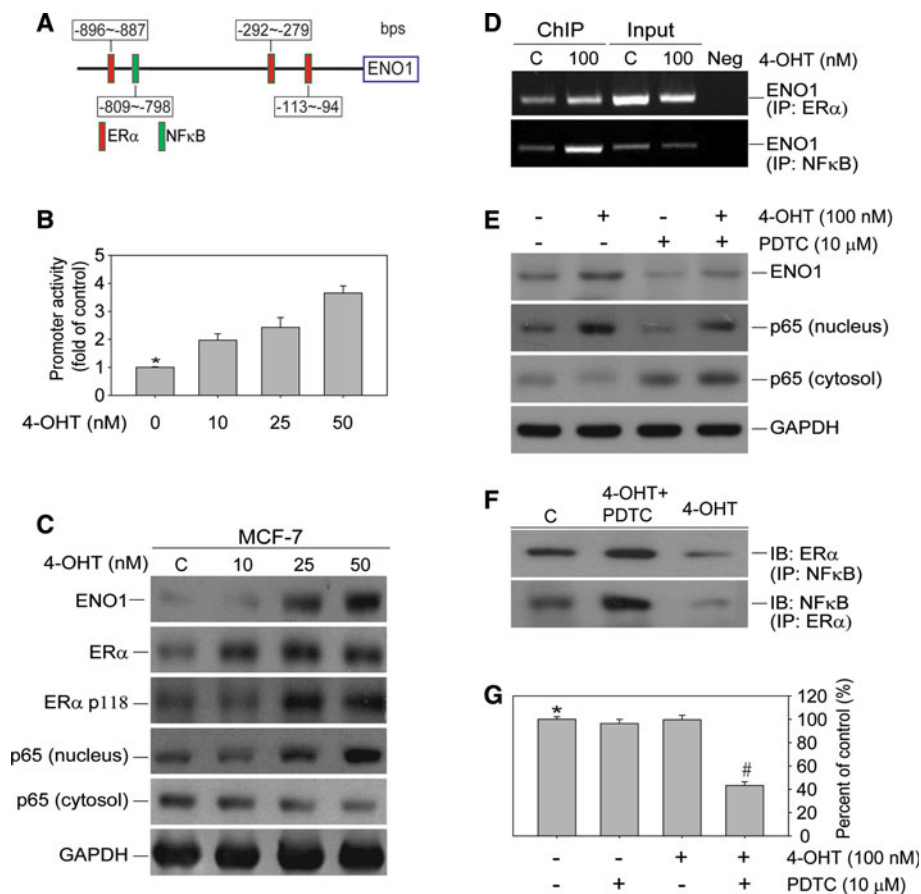


Fig. 5 ER α and NF κ B are involved in 4-OHT-induced ENO-1 transcriptional regulation. **a** Schematic representation of the ENO-1 promoter region ($-1,036/-1$) illustrating the putative ER α and NF κ B transcription factors binding sites. **b** MCF-7 cells were transiently transfected with 2 μ g of pGL3(ENO-1) and 500 ng of pRL-TK plasmid for 24 h and then treated with 4-OHT for an additional 24 h. Cell lysates were harvested, and firefly and *Renilla* luciferase activities were measured with a 96-well luminometer (Hidex Chameleon, Finland). Relative luciferase units were normalized to renilla luciferase from the same cell lysates. Luciferase activity obtained from the PGL3(ENO-1) reporter plasmid-transfected cells without 4-OHT treatment was defined as 100%. Data indicate the mean fold ratios of ENO-1 promoter activity compared between vehicle (0.1% ethanol)- and 4-OHT-treated cells; error bars are 95% confidence intervals. Data were analyzed using paired *t*-tests; all *P*-values are two-sided. The comparisons were carried out as follows: vehicle vs. 4-OHT (10 nM), $*P = 0.032$; vehicle vs. 4-OHT (25 nM), $*P = 0.025$; vehicle vs. 4-OHT (50 nM), $*P = 0.011$. ($n = 3$ per group). **c** MCF-7 cells were treated with the indicated concentrations of 4-OHT for 24 h. ENO-1, ER α , the activated form of ER α (ER α -p118), and nuclear and cytosolic NF κ B (p65) protein levels were detected by immunoblot analysis with antigen-specific antibodies. Cells were treated with ethanol (0.1%, v/v) as a vehicle control (indicated as c). **d** ChIP assays were performed for MCF-7 cells

treated with 4-OHT (100 nM) for 24 h. The data shown are representative of three independent experiments with similar results. The genomic DNA isolated from MCF-7 was used as a positive input control to ascertain the PCR conditions. Neg, negative control. **e** Tam-R cells were pretreated with PDTC for 2 h, and then treated in the presence or absence of 4-OHT for an additional 24 h. Immunoblotting analysis was performed, and the protein levels of ENO-1 and NF κ B (p65, nuclear and cytosolic forms) were detected. **f** Protein interactions between NF κ B and ER α in the cytosolic fraction of 4-OHT (100 nM for 24 h)-treated and 4-OHT + PDTC (10 μ M)-treated Tam-R cells were detected by co-immunoprecipitation analysis. NF κ B (p65) and ER α were immunoprecipitated (IP) using specific antibodies, as indicated. Precipitated proteins were further visualized by immunoblot analysis (IB) using the indicated antibodies. C, cytosolic fraction of untreated Tam-R cell lysates was used as a control. **g** Tam-R cells were pretreated with PDTC for 2 h and then treated in the presence or absence of 4-OHT for an additional 24 h. Cell viability was assessed by MTT, as described in the “Materials and methods” section. Data are presented as means of at least three samples in each group; error bars are 95% confidence intervals. Data were analyzed using paired *t*-tests; all *P*-values are two-sided. The comparison was performed in Tam-R cells exposed to: ethanol vs. PDTC, $*P = 0.73$, ethanol vs. 4-OHT + PDTC, $*P = 0.012$, ethanol vs. 4-OHT, $P = 0.89$, or PDTC vs. 4-OHT + PDTC, $\#P = 0.013$

potentiated 4-OHT-induced antiproliferative effects (Fig. 4d). We wondered whether blocking ENO-1 transcriptional regulation could sensitize Tam-R cells to 4-OHT treatment (Fig. 6b). To test this hypothesis, we pretreated Tam-R cells with an NF κ B nuclear translocation inhibitor

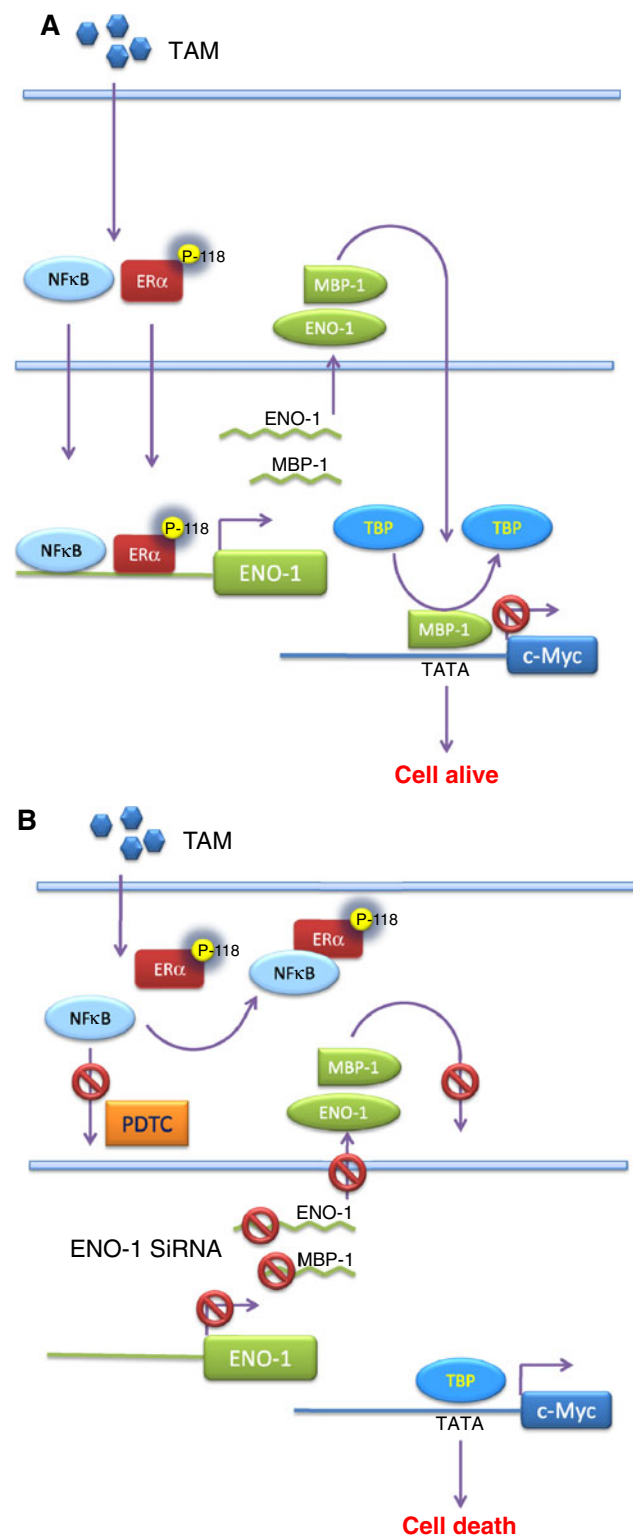
(PDTC), and then exposed these cells to 4-OHT for an additional 24 h, after which immunoblotting was performed. Increased retention of NF κ B (p65) in the cytosolic fractions was detected in cells with PDTC plus 4-OHT treatment (Fig. 5e, lane 4). Interestingly, 4-OHT-induced ENO-1

Fig. 6 Schematic diagram of the signaling pathways involved in 4-OHT-induced ENO-1 overexpression, which results in endocrine resistance in human breast cancer (MCF-7) cells. **a** ENO-1 was induced by 4-OHT treatment through transcriptional upregulation of ER α and NF κ B. The excess expression of ENO-1 and its translated form (MBP-1) exert a negative regulatory effect on c-Myc transcription that counteracts the 4-OHT-induced apoptosis of breast cancer cells [15, 29, 30]. Therefore, we hypothesize that downregulation of c-Myc by either ENO-1 or MBP-1 may be a mechanism by which breast cancer cells acquire resistance to tamoxifen therapy. **b** In contrast, inhibition of ENO-1 transcriptional regulation either by blocking the NF κ B signal pathway or by siRNA knockdown significantly sensitized human breast cancer cells to 4-OHT-induced cytotoxicity. These results suggest that ENO-1 may facilitate resistance to 4-OHT-induced cell death and that the combined use of 4-OHT and an NF κ B pathway inhibitor (PDTC) may provide a novel approach to overcome tamoxifen resistance in breast cancer

protein expression was almost completely attenuated by PDTC pretreatment (Fig. 5e, lanes 2 vs. 4). One possible explanation has been described in previous studies demonstrating that increased retention of NF κ B in the cytoplasm antagonizes ER α -mediated biological functions through the formation of a protein complex [36, 37]. Protein interactions between NF κ B and ER α in the cytosolic fraction of 4-OHT + PDTC-treated Tam-R cells were detected by co-immunoprecipitation, while increased levels of the cytosolic NF κ B/ER α protein complex were found in Tam-R cells treated with 4-OHT + PDTC compared to those treated with 4-OHT alone (Fig. 5f, lanes 2 vs. 3). Under the same treatment conditions, pretreatment with PDTC significantly enhanced the cytotoxic effects of 4-OHT in Tam-R cells, as determined by cell proliferation assays (Fig. 5g, lane 4, * $P = 0.012$). These results may explain previous findings that therapeutic inhibition of NF κ B activation improves endocrine responsiveness in high-risk ER-positive breast cancers [38, 39].

Discussion

Estrogens and the ER are implicated in breast cancer progression and are thus targets of hormonal therapies such as aromatase inhibitors (AI), which block estrogen production, and antiestrogens like tamoxifen, which target the ER [40]. Thus, targeting the estrogen receptor pathway is a valid, effective, biologically based therapy for breast cancer. However, a significant proportion of patients with ER-positive tumors do not have sustained objective responses, and many who possess these responses initially relapse subsequently due to the acquisition of endocrine resistance [41]. On the other hand, it is widely recognized that HER-2-positive tumors generally have a more aggressive phenotype than HER-2-negative tumors as reflected by the patients' poor response to 4-OHT therapy [42]. It has been reported previously that, in those patients who have ER-positive and HER-2-positive cancers, the mean concentration of ER in



the tumor is lower than in those tumors that are HER-2-negative [43]. This finding is particularly significant for this study, because we found that high expression of ENO-1 was preferentially detected in ER-positive/HER-2-negative tumors. Thus, it is important to consider the possibility that

ENO-1 overexpression may be associated with higher ER values rather than HER-2 negativity per se.

In this study, we have attempted to minimize these problems by (a) selecting an entirely ER-positive group of patients; (b) conducting LCM plus real-time PCR analysis to confirm any detected ENO-1 mRNA overexpression in tumor lesions; and (c) conducting the study in primary disease in which the 4-OHT therapeutic response can be assessed in the same patients as the ENO-1 measurement. A novel aspect of the study was the assessment of the biological response, including the disease-free interval, dominant site of relapse, nodal status, tumor size, and tumor grade (Table 1). In addition, no other study provides molecular evidence to explain such observations. Our in vitro results indicate that ENO-1 mRNA overexpression was significantly induced by long-term, noncytotoxic concentrations of 4-OHT (100 nM) treatment, after which 4-OHT therapeutic resistant (Tam-R) cells were established [44]. Inhibition of ENO-1 mRNA expression significantly enhanced the 4-OHT-induced cytotoxic effect on Tam-R cell growth. Our in vivo and in vitro observations imply that overexpression of ENO-1 conferred 4-OHT-induced drug resistance.

ENO-1 is a key glycolytic enzyme that has been used as a diagnostic marker to identify human lung cancers [22–24]. Recent research has shown that specific inhibitors of key glycolytic enzymes may enhance the activity of anti-cancer drugs [45, 46]. Furthermore, extensive trials have indicated that cancer cells with high glycolytic activity exhibit decreased sensitivity to anticancer agents [47]. In the present study, the mRNA levels of ENO-1 were higher in tumor cells than in normal clustered cells dissected from either surgical or LCM samples. We found an intimate relationship between ENO-1 and ER α expression and demonstrated for the first time that ENO-1 is transcriptionally upregulated by NF κ B and ER α at lower concentrations (10–50 nM) of 4-OHT (Fig. 5). Similar results were also found in another proteomic study, in which the ENO-1 protein was induced by E2 treatment in MCF-7 cells [48]. However, the role of increased ENO-1 expression induced by E2- or 4-OHT treatment in tumor cells was not clearly investigated. One possible hypothesis suggests that ENO-1 stimulates tumor growth by supporting an increased metabolic rate in tumor cells. Such effects play an important role in breast cancer dormancy, promoting the survival of cancer cells in metastatic foci by counteracting proapoptotic signals in the microenvironment [49]. Elevated ENO-1 expression resulted in the presence of high titer levels of antibodies in the sera of breast cancer patients with visual impairments and electrophysiological abnormalities that are characteristic of cancer-associated retinopathy [50]. These data suggest that anti-ENO-1 antibodies could be responsible for the development of

cancer-associated symptoms, which impair the therapeutic effects of 4-OHT in breast tumor patients. In the present study, we hypothesized that intracellular ENO-1 could modulate c-Myc protein expression, thereby leading to the acquisition of resistance to 4-OHT therapy by the breast cancer cells (Fig. 6a). Such a hypothesis has been reported by previous studies, which have demonstrated that overexpression of ENO-1 and its translated form (MBP-1) inhibit c-Myc transcription [15, 30]. Therefore, we explored here whether inhibition of ENO-1 expression, either through the interruption of NF κ B signaling pathways by PDTC or by SiRNA knockdown, enhances the sensitivity of tumor cells to 4-OHT treatment (Figs. 4d and 5g). The results described above support our hypothesis and may help to determine a novel technique for overcoming 4-OHT resistance in breast cancer therapy.

Acknowledgments This study was supported by the National Science Council, grant NSC 95-2320-B-038-016-MY3 for Dr. Ho, and NSC 96-2314-B-038-002 for Dr. Wu, and by the Cathay Medical Center (95CGH-TMU-09 and 96CGH-TMU-05).

References

1. Jemal A, Murray T, Ward E, Samuels A, Tiwari RC, Ghafoor A, Feuer EJ, Thun MJ (2005) Cancer statistics, 2005. *CA Cancer J Clin* 55:10–30
2. Dodwell D, Williamson D (2008) Beyond tamoxifen: extended and late extended endocrine therapy in postmenopausal early breast cancer. *Cancer Treat Rev* 34:137–144
3. Jaiyesimi IA, Buzdar AU, Decker DA, Hortobagyi GN (1995) Use of tamoxifen for breast cancer: twenty-eight years later. *J Clin Oncol* 13:513–529
4. Chen B, Wang Y, Kane SE, Chen S (2008) Improvement of sensitivity to tamoxifen in estrogen receptor-positive and Herceptin-resistant breast cancer cells. *J Mol Endocrinol* 41:367–377
5. Kim SK, Yang JW, Kim MR, Roh SH, Kim HG, Lee KY, Jeong HG, Kang KW (2008) Increased expression of Nrf2/ARE-dependent anti-oxidant proteins in tamoxifen-resistant breast cancer cells. *Free Radic Biol Med* 45:537–546
6. Masri S, Phung S, Wang X, Wu X, Yuan YC, Wagman L, Chen S (2008) Genome-wide analysis of aromatase inhibitor-resistant, tamoxifen-resistant, and long-term estrogen-deprived cells reveals a role for estrogen receptor. *Cancer Res* 68:4910–4918
7. Honorat M, Mesnier A, Vendrell J, Guitton J, Bieche I, Lidereau R, Kruh GD, Dumontet C, Cohen P, Payen L (2008) ABCC11 expression is regulated by estrogen in MCF7 cells, correlated with estrogen receptor alpha expression in postmenopausal breast tumors and overexpressed in tamoxifen-resistant breast cancer cells. *Endocr Relat Cancer* 15:125–138
8. Lebioda L, Stec B (1988) Crystal structure of enolase indicates that enolase and pyruvate kinase evolved from a common ancestor. *Nature* 333:683–686
9. Chi-Shing Cho W (2007) Potentially useful biomarkers for the diagnosis, treatment and prognosis of lung cancer. *Biomed Pharmacother* 61:515–519
10. Horiatis D, Wang Q, Pinski J (2004) A new screening system for proliferation-independent anti-cancer agents. *Cancer Lett* 210: 119–124

11. Riby JE, Firestone GL, Bjeldanes LF (2008) 3', 3'-diindolylmethane reduces levels of HIF-1 α and HIF-1 activity in hypoxic cultured human cancer cells. *Biochem Pharmacol* 75:1858–1867
12. Sims PA, Menefee AL, Larsen TM, Mansoorabadi SO, Reed GH (2006) Structure and catalytic properties of an engineered heterodimer of enolase composed of one active and one inactive subunit. *J Mol Biol* 355:422–431
13. Chang YS, Wu W, Walsh G, Hong WK, Mao L (2003) Enolase- α is frequently down-regulated in non-small cell lung cancer and predicts aggressive biological behavior. *Clin Cancer Res* 9:3641–3644
14. Ray R, Miller DM (1991) Cloning and characterization of a human c-myc promoter-binding protein. *Mol Cell Biol* 11:2154–2161
15. Subramanian A, Miller DM (2000) Structural analysis of alpha-enolase. Mapping the functional domains involved in down-regulation of the c-myc protooncogene. *J Biol Chem* 275:5958–5965
16. Fan P, Wang J, Santen RJ, Yue W (2007) Long-term treatment with tamoxifen facilitates translocation of estrogen receptor α out of the nucleus and enhances its interaction with EGFR in MCF-7 breast cancer cells. *Cancer Res* 67:1352–1360
17. Aerts JL, Gonzales MI, Topalian SL (2004) Selection of appropriate control genes to assess expression of tumor antigens using real-time RT-PCR. *Biotechniques* 36:84–86, 88, 90–91
18. Chen F, Kim E, Wang CC, Harrison LE (2005) Ciglitazone-induced p27 gene transcriptional activity is mediated through Sp1 and is negatively regulated by the MAPK signaling pathway. *Cellular signalling* 17:1572–1577
19. Chen CS, Wu CH, Lai YC, Lee WS, Chen HM, Chen RJ, Chen LC, Ho YS, Wang YJ (2008) NF- κ B-activated tissue transglutaminase is involved in ethanol-induced hepatic injury and the possible role of propolis in preventing fibrogenesis. *Toxicology* 246:148–157
20. Finak G, Bertos N, Pepin F, Sadekova S, Souleimanova M, Zhao H, Chen H, Omeroglu G, Meterissian S, Omeroglu A, Hallett M, Park M (2008) Stromal gene expression predicts clinical outcome in breast cancer. *Nat Med* 14:518–527
21. Wilkinson DS, Ogden SK, Stratton SA, Piechan JL, Nguyen TT, Smulian GA, Barton MC (2005) A direct intersection between p53 and transforming growth factor beta pathways targets chromatin modification and transcription repression of the alpha-fetoprotein gene. *Molecular and cellular biology* 25:1200–1212
22. Tiseo M, Ardizzoni A, Cafferata MA, Loprevite M, Chiaromondia M, Filiberti R, Marroni P, Grossi F, Paganuzzi M (2008) Predictive and prognostic significance of neuron-specific enolase (NSE) in non-small cell lung cancer. *Anticancer Res* 28:507–513
23. He P, Naka T, Serada S, Fujimoto M, Tanaka T, Hashimoto S, Shima Y, Yamadori T, Suzuki H, Hirashima T, Matsui K, Shiono H, Okumura M, Nishida T, Tachibana I, Norioka N, Norioka S, Kawase I (2007) Proteomics-based identification of alpha-enolase as a tumor antigen in non-small lung cancer. *Cancer Sci* 98:1234–1240
24. Chang GC, Liu KJ, Hsieh CL, Hu TS, Charoenfuprasert S, Liu HK, Luh KT, Hsu LH, Wu CW, Ting CC, Chen CY, Chen KC, Yang TY, Chou TY, Wang WH, Whang-Peng J, Shih NY (2006) Identification of alpha-enolase as an autoantigen in lung cancer: its overexpression is associated with clinical outcomes. *Clin Cancer Res* 12:5746–5754
25. Panasci L, Jean-Claude BJ, Vasilescu D, Mustafa A, Damian S, Damian Z, Georges E, Liu Z, Batist G, Leyland-Jones B (1996) Sensitization to doxorubicin resistance in breast cancer cell lines by tamoxifen and megestrol acetate. *Biochem Pharmacol* 52:1097–1102
26. Lavie Y, Cao H, Volner A, Lucci A, Han TY, Geffen V, Giuliano AE, Cabot MC (1997) Agents that reverse multidrug resistance, tamoxifen, verapamil, and cyclosporin A, block glycosphingolipid metabolism by inhibiting ceramide glycosylation in human cancer cells. *J Biol Chem* 272:1682–1687
27. Fujita T, Washio K, Takabatake D, Takahashi H, Yoshitomi S, Tsukuda K, Ishibe Y, Ogasawara Y, Doihara H, Shimizu N (2005) Proteasome inhibitors can alter the signaling pathways and attenuate the P-glycoprotein-mediated multidrug resistance. *Int J Cancer* 117:670–682
28. Ho YS, Duh JS, Jeng JH, Wang YJ, Liang YC, Lin CH, Tseng CJ, Yu CF, Chen RJ, Lin JK (2001) Griseofulvin potentiates antitumorigenesis effects of nocodazole through induction of apoptosis and G2/M cell cycle arrest in human colorectal cancer cells. *Int J Cancer* 91:393–401
29. Hermeking H, Eick D (1994) Mediation of c-Myc-induced apoptosis by p53. *Science* 265:2091–2093
30. Ray RB, Steele R, Seftor E, Hendrix M (1995) Human breast carcinoma cells transfected with the gene encoding a c-myc promoter-binding protein (MBP-1) inhibits tumors in nude mice. *Cancer Res* 55:3747–3751
31. Kang Y, Cortina R, Perry RR (1996) Role of c-myc in tamoxifen-induced apoptosis estrogen-independent breast cancer cells. *J Natl Cancer Inst* 88:279–284
32. Mandlekar S, Kong AN (2001) Mechanisms of tamoxifen-induced apoptosis. *Apoptosis* 6:469–477
33. Planas-Silva MD, Hamilton KN (2007) Targeting c-Src kinase enhances tamoxifen's inhibitory effect on cell growth by modulating expression of cell cycle and survival proteins. *Cancer Chemother Pharmacol* 60:535–543
34. Zheng A, Kallio A, Harkonen P (2007) Tamoxifen-induced rapid death of MCF-7 breast cancer cells is mediated via extracellularly signal-regulated kinase signaling and can be abrogated by estrogen. *Endocrinology* 148:2764–2777
35. Webb P, Lopez GN, Uht RM, Kushner PJ (1995) Tamoxifen activation of the estrogen receptor/AP-1 pathway: potential origin for the cell-specific estrogen-like effects of antiestrogens. *Mol Endocrinol* 9:443–456
36. Vendrell JA, Bieche I, Desmetz C, Badia E, Tozlu S, Nguyen C, Nicolas JC, Lidereau R, Cohen PA (2005) Molecular changes associated with the agonist activity of hydroxy-tamoxifen and the hyper-response to estradiol in hydroxy-tamoxifen-resistant breast cancer cell lines. *Endocr Relat Cancer* 12:75–92
37. Quaeadackers ME, van den Brink CE, van der Saag PT, Tertoolen LG (2007) Direct interaction between estrogen receptor α and NF- κ B in the nucleus of living cells. *Mol Cell Endocrinol* 273:42–50
38. Kalaitzidis D, Gilmore TD (2005) Transcription factor cross-talk: the estrogen receptor and NF- κ B. *Trends Endocrinol Metab* 16:46–52
39. Zhou Y, Eppenberger-Castori S, Marx C, Yau C, Scott GK, Eppenberger U, Benz CC (2005) Activation of nuclear factor- κ B (NF κ B) identifies a high-risk subset of hormone-dependent breast cancers. *Int J Biochem Cell Biol* 37:1130–1144
40. Harvell DM, Richer JK, Singh M, Spoelstra N, Finlayson C, Borges VF, Elias AD, Horwitz KB (2008) Estrogen regulated gene expression in response to neoadjuvant endocrine therapy of breast cancers: tamoxifen agonist effects dominate in the presence of an aromatase inhibitor. *Breast Cancer Res Treat* 112:489–501
41. Ali S, Coombes RC (2002) Endocrine-responsive breast cancer and strategies for combating resistance. *Nat Rev Cancer* 2:101–112
42. Slamon DJ, Godolphin W, Jones LA, Holt JA, Wong SG, Keith DE, Levin WJ, Stuart SG, Udove J, Ullrich A et al (1989) Studies of the HER-2/neu proto-oncogene in human breast and ovarian cancer. *Science* 244:707–712
43. Elledge RM, Green S, Ciocca D, Pugh R, Allred DC, Clark GM, Hill J, Ravdin P, O'Sullivan J, Martino S, Osborne CK (1998) HER-2 expression and response to tamoxifen in estrogen

- receptor-positive breast cancer: a southwest oncology group study. *Clin Cancer Res* 4:7–12
44. John S, Nayvelt I, Hsu HC, Yang P, Liu W, Das GM, Thomas T, Thomas TJ (2008) Regulation of estrogenic effects by beclin 1 in breast cancer cells. *Cancer Res* 68:7855–7863
 45. Peng QP, Zhou JM, Zhou Q, Pan F, Zhong DP, Liang HJ (2008) Downregulation of the hexokinase II gene sensitizes human colon cancer cells to 5-fluorouracil. *Chemotherapy* 54:357–363
 46. Scatena R, Bottoni P, Pontoglio A, Mastrototaro L, Giardina B (2008) Glycolytic enzyme inhibitors in cancer treatment. *Expert Opin Investig Drugs* 17:1533–1545
 47. Christofk HR, Vander Heiden MG, Harris MH, Ramanathan A, Gerszten RE, Wei R, Fleming MD, Schreiber SL, Cantley LC (2008) The M2 splice isoform of pyruvate kinase is important for cancer metabolism and tumour growth. *Nature* 452:230–233
 48. Malorni L, Cacace G, Cuccurullo M, Pocsfalvi G, Chambery A, Farina A, Di Maro A, Parente A, Malorni A (2006) Proteomic analysis of MCF-7 breast cancer cell line exposed to mitogenic concentration of 17beta-estradiol. *Proteomics* 6:5973–5982
 49. Zhang D, Tai LK, Wong LL, Chiu LL, Sethi SK, Koay ES (2005) Proteomic study reveals that proteins involved in metabolic and detoxification pathways are highly expressed in HER-2/neu-positive breast cancer. *Mol Cell Proteomics* 4:1686–1696
 50. Ejma M, Misiuk-Hojlo M, Gorczyca WA, Podemski R, Szymaniec S, Kuropatwa M, Rogozinska-Szczepka J, Bartnik W (2008) Antibodies to 46-kDa retinal antigen in a patient with breast carcinoma and cancer-associated retinopathy. *Breast Cancer Res Treat* 110:269–271